Friction **5**(3): 339–350 (2017)
https://doi.org/10.1007/s40544-017-0179-1
ISSN 2223-7690
CN 10-1237/TH

RESEARCH ARTICLE

Combined effect of surface microgeometry and adhesion in normal and sliding contacts of elastic bodies

Irina GORYACHEVA*, Yulia MAKHOVSKAYA

Institute for Problems in Mechanics of the Russian Academy of Sciences, Pr. Vernadskogo 101-1, Moscow 119526, Russia

Received: 28 April 2017 / Revised: 06 June 2017 / Accepted: 19 June 2017

Abstract: In this study, models are proposed to analyze the combined effect of surface microgeometry and adhesion on the load–distance dependence and energy dissipation in an approach–separation cycle, as well as on the formation and rupture of adhesive bridges during friction. The models are based on the Maugis–Dugdale approximation in normal and frictional (sliding and rolling) contacts of elastic bodies with regular surface relief. For the normal adhesive contact of surfaces with regular relief, an analytical solution, which takes into account the mutual effect of asperities, is presented. The contribution of adhesive hysteresis into the sliding and rolling friction forces is calculated for various values of nominal pressure, parameters of microgeometry, and adhesion.

Keywords: adhesion; roughness; discrete contact; rolling friction; sliding friction

1 Introduction

Adhesive interactions play a very important role in surface friction, particularly at micro and nanoscale levels [1, 2]. It was established experimentally and theoretically that at these scale levels, the contact characteristics and friction forces depend on the mechanical properties of the interacting bodies, their surface energy, and surface microgeometry.

Theoretical models that have been developed to analyze the adhesion during contact of deformable bodies differ in constitutive equations for solids, models of adhesive interaction, and description of the geometry of contacting surfaces. The commonly used models of adhesive interaction include the classical JKR [3] and DMT [4] theories, Maugis–Dugdale model [5], exact form of the Lennard–Jones potential [6] as well as its approximations by various analytical functions [7], double-Hertz approximation [8], and piecewise-constant approximation [9]. The geometry of interacting surfaces can be described as a set of asperities of determined configuration, or it can be modeled by statistical or fractal approaches. All these models and approaches being combined in the formulation of a contact problem have generated a large number of theoretical works, each having a specific limit and applicability area.

The normal adhesive contact between rough elastic bodies was first studied by Johnson [10] and Fuller and Tabor [11], who employed exponential and Gaussian distributions of heights of asperities, respectively, and the JKR model of adhesion. It was shown that large diversity of heights of asperities leads to low adhesion between the surfaces, because high asperities coming into contact can cause elastic forces of repulsion between the surfaces. The DMT model of adhesion was generalized for the case of a rough surface with a specified distribution of heights in Ref. [12]. The method suggested by Fuller and Tabor [11] was applied in Ref. [13] to describe a rough contact with the use of the Maugis–Dugdale model. The adhesion of rough elastic bodies with arbitrary nominal geometry at macrolevel was modeled in Ref. [14] by applying a statistical description of roughness at microlevel and the JKR and DMT models of adhesion. The models of adhesive contact developed by Rumpf [15] and Rabinovich et al. [16] consider rigid rough surfaces

* Corresponding author: Irina GORYACHEVA, E-mail: goryache@ipmnet.ru

having hemispherical asperities, whose centers lie on the surfaces (small asperities superimposed on large asperities), and both models use the Derjaguin approximation for adhesive interaction [17] (see the discussion on Derjaguin approximation in Ref. [18]).

There were several studies that considered normal contact between rough surfaces with adhesion by using a fractal approach. Following are several examples. A contact problem between self-affine fractal surfaces was studied using a method of dimensionality reduction in Ref. [19]. The fractal approach was also employed in Ref. [20] for studying adhesive contact between rough surfaces. An approach similar to fractal surface roughness description was used by Persson and Tossati with the JKR [21, 22] and DMT [23] models of adhesion. A model for adhesion between self-affine rough surfaces based on the JKR theory was suggested by Ciavarella [24] for a contact close to saturation. A numerical simulation of adhesion for self-affine rough surfaces was carried out in Ref. [25]. The results of this simulation and the applicability area of the DMT approximation in rough adhesive contacts were discussed in Refs. [26, 27]. A simplified model for adhesion between elastic rough solids with Gaussian multiple scales of roughness was suggested in Ref. [28]. The limitations of the fractal approach to describe the roughness of real surfaces were discussed by Borodich et al. [29, 30].

To analyze the effect of the shape of asperities and their mutual arrangement, it is necessary to consider contact problems for surfaces with regular relief. Periodic formulations of contact problems often allow a closed-form solution, which takes into account the mutual effect of contact spots through the elastic body. Two-dimensional contact problems for a rough surface with periodic relief and an elastic half-plane were solved [31–33] for various models of adhesion. For a 3D case, the adhesive contact between a periodic system of asperities and elastic half-space was modeled in Ref. [34] by using the Maugis–Dugdale approximation and by considering the shape of asperities and mutual effect of contact spots.

According to the classical approach [35], the sliding friction force is the sum of two components: mechanical component and adhesive component. The adhesive component is assumed to be equal to the force required for plastic shear to occur on the microcontacts. This approach to modeling the adhesion component of the friction force was developed in Refs. [36–38]. However, it is known that adhesion can contribute to the friction force even in the absence of plastic deformation, e.g., at very small loads. To model the adhesion friction force in this case, an approach is developed by considering the adhesion contact as opening and closing cracks [39]. It was established experimentally that the value of the friction force between two solids correlates with the value of adhesion hysteresis in an approach–separation cycle of these solids [40–42]. Models relating adhesion friction force to adhesion hysteresis were suggested for a cylinder [43] and a periodic rough surface [44] sliding on an elastic body. Adhesion hysteresis was taken into account as the difference in the surface energy before and after the moving contact zone. Another approach was suggested by Heise and Popov [45], who calculated the sliding friction force between two rough surfaces as a result of adhesion hysteresis in the approach–separation cycle for asperities. They used the JKR model of adhesion and random distribution of heights of asperities. In Ref. [46], the adhesion component of the sliding friction force was modeled by calculating the energy dissipation in the formation and rupture of the adhesive contacts between asperities of rough surfaces in sliding. In this model, rough surfaces had regular relief and the Maugis–Dugdale model of adhesion was used, making it possible to apply the solution in a wide range of geometric and adhesive characteristics.

Adhesive interactions also contribute into the rolling resistance [1]. The adhesive component of the rolling resistance was calculated in Ref. [1] based on the assumption that each approach and separation of molecules is accompanied by an energy loss. In Ref. [47], the rolling resistance was accounted for by the attraction of separating parts of the surfaces owing to the opposite electrical charges arising between them. The adhesive component of the rolling resistance was calculated in Ref. [48] based on the energy dissipation mechanism in the approaching and separation of asperities of contacting surfaces in the process of rolling.

The present study focuses on the analysis of the effect of adhesive interaction modeled by the Maugis–Dugdale approximation in normal and frictional (sliding

and rolling) contacts of elastic bodies with regular surface relief. The combined effect of adhesion and surface microgeometry on the load–distance dependence and energy dissipation in the approach–separation cycle, as well as on the formation and rupture of adhesive bridges during friction is analyzed. For the normal adhesive contact of surfaces with regular relief, an analytical solution that takes into account the mutual effect of asperities is presented.

2 Normal contact of a rough surface with elastic half-space in the presence of adhesion

2.1 Model of adhesion

The adhesive force per unit area $p_a(z)$ is approximated by a piecewise constant function known as the Maugis–Dugdale model [5]:

$$p_a(z)=\begin{cases}-p_0, & 0<z\le h_0\\ 0, & z>h_0\end{cases} \tag{1}$$

In this case, the work of adhesion w is defined by

$$w=\int_0^\infty p_a(z)\,\mathrm{d}z=p_0h_0 \tag{2}$$

For a spherical punch in contact with an elastic half-space, the model of adhesion as defined by Eqs. (1)–(2), provides a closed-form solution [5]. Unlike the classical models of adhesion, i.e., the JKR [3] and DMT [4] models, the Maugis–Dugdale model is applicable to solids of arbitrary stiffness in a wide range of adhesion parameters.

2.2 Problem formulation

We consider the interaction of two solids with nominally flat surfaces (Fig. 1). Solid 1 is rigid and is covered with rigid hemispherical asperities of equal radius R, while solid 2 is an elastic half-space with a smooth surface. We assume that the asperities are in the nodes of a hexagonal lattice with a lattice spacing l. The origin of the local cylindrical system of coordinates (r, z, ϕ) coincides with the point at which an asperity touches the undeformed half-space. The z-axis is directed into the half-space. In this system of coordinates, the shape of each asperity is described by the function $f(r)=r^2/(2R)$.

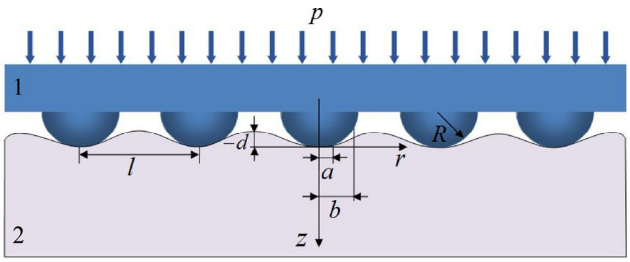

Fig. 1 Contact scheme between a rigid rough surface and an elastic half-space in the presence of adhesion.

Solid 1 is acted upon by a uniform nominal pressure p. The distributions of pressure and elastic displacement of the boundary of the half-space are assumed to be axisymmetric near each asperity. The gap between the contacting surfaces near an asperity can be represented as

$$h(r)=f(r)-f(a)+u(r)-u(a) \tag{3}$$

where $u(r)$ is the elastic displacement of the boundary of the half-space in the z direction, and a is the radius of the contact spot.

To take into account the adhesive attraction between the surfaces, we use the Maugis–Dugdale model defined by Eqs. (1)–(2) and assume that a negative pressure $(-p_0)$ is applied to the elastic half-space in the ring-shaped region $a\le r\le b$ around each asperity. From Eq. (2), we obtain the relation for the gap at $r=b$:

$$h(b)=\frac{w}{p_0} \tag{4}$$

The values of the work of adhesion w and adhesive pressure p_0 are assumed to be known.

The problem is solved by the method of localization [49]. In accordance to this method, to determine the stress–strain state near a contact spot, one should replace the effect of the remaining contact spots by the action of an averaged pressure in the region $r\ge R_{\mathrm{eff}}$. The solution to this problem was established in Ref. [34] for a system of asperities, whose shape is described by the power-law function of an even degree. We will use the results obtained in Ref. [34] for the case of asperities of hemispherical shape.

If the surfaces are in contact, the following relations

for the nominal pressure p and distance d between the surfaces are valid:

$$p=\frac{\pi}{\sqrt{3}l^2}\frac{4E^*a^3/(3R)-2p_0b^2\left(\arccos(a/b)+a\sqrt{1-(a/b)^2}\Big/b\right)}{\arccos(a/R_{\text{eff}})+a\sqrt{1-(a/R_{\text{eff}})^2}\Big/R_{\text{eff}}} \tag{5}$$

$$d=-\frac{a^2}{R}+\frac{2p_0b}{E^*}\sqrt{1-\left(\frac{a}{b}\right)^2}+\frac{2pR_{\text{eff}}}{E^*}\sqrt{1-\left(\frac{a}{R_{\text{eff}}}\right)^2} \tag{6}$$

The contact radius a and the external radius of the region of adhesion b are related by the equation that follows from Eqs. (3)–(4) and has the form

$$h(b)=\left(\frac{b^2}{2R}-d\right)\frac{2}{\pi}\arccos\frac{a}{b}+\frac{a^2}{\pi R}\sqrt{\left(\frac{b}{a}\right)^2-1}-\frac{4p_0}{\pi E^*}(b-a)-\frac{4pR_{\text{eff}}}{\pi E^*}\left[E\left(\frac{b}{R_{\text{eff}}}\right)-E\left(\arcsin\frac{a}{b},\frac{b}{R_{\text{eff}}}\right)\right]=\frac{w}{p_0} \tag{7}$$

where $E(x), E(\theta,x)$ are complete and incomplete elliptic integrals of the second kind, respectively. In Eqs. (5)–(7), we use the notation $E^*=E/(1-\nu^2)$, where E and ν are the Young's modulus and Poisson's ratio of the elastic half-space, respectively, and $R_{\text{eff}}=l(\sqrt{3}/(2\pi))^{1/2}$.

If the surfaces are not in contact and they interact only by adhesive forces, the nominal pressure and distance are defined by

$$p=-\frac{2\pi p_0b^2}{\sqrt{3}l^2},\quad d=-\frac{b^2}{2R}+\frac{4}{\pi E^*}p_0b\left[1-\frac{b}{R_{\text{eff}}}E\left(\frac{b}{R_{\text{eff}}}\right)\right]+\frac{w}{p_0} \tag{8}$$

The solution specified by Eqs. (5)–(8) is applicable for $l>b$.

If q is the normal force acting on each asperity, then from the geometry of the problem it follows that

$$p=\frac{2q}{\sqrt{3}l^2} \tag{9}$$

From Eqs. (5)–(7), by taking into account Eq. (9) and setting $l\to\infty$, we obtain the solution to the contact problem for an individual hemispherical asperity of radius R acted upon by a normal load q and an elastic half-space:

$$q=\frac{4E^*}{3}\frac{a^3}{R}-2p_0b^2\left(\arccos\frac{a}{b}+\frac{a}{b}\sqrt{1-\left(\frac{a}{b}\right)^2}\right),\quad d=-\frac{a^2}{R}+\frac{2p_0b}{E^*}\sqrt{1-\left(\frac{a}{b}\right)^2} \tag{10}$$

$$\left(\frac{b^2}{2R}-d\right)\frac{2}{\pi}\arccos\frac{a}{b}+\frac{a^2}{\pi R}\sqrt{\left(\frac{b}{a}\right)^2-1}-\frac{4p_0}{\pi E^*}(b-a)=\frac{w}{p_0} \tag{11}$$

Eqs. (9)–(10) coincide with the solution obtained by Maugis [5].

For the case where an individual asperity interacts with the elastic half-space without contact, from Eqs. (8) and (9) for $l\to\infty$ we have

$$q=-\pi b^2p_0,\quad d=-\frac{b^2}{2R}+\frac{4}{\pi E^*}p_0b+\frac{w}{p_0} \tag{12}$$

2.3 Parametrization

For convenience in the calculation and analysis of results, we use the following parametrization by introducing a dimensionless nominal pressure p^* and dimensionless distance between the surfaces d^* in accordance with the following relations:

$$p^*=\frac{l^2}{\sqrt{3}\pi w\ R}p,\quad d^*=\frac{4}{3}\left(\frac{E^{*2}}{\pi^2w^2R}\right)^{1/3}d \tag{13}$$

The solution to the problem depends on the following two dimensionless parameters:

$$\lambda=p_0\left(\frac{9R}{2\pi wE^{*2}}\right)^{1/3} \tag{14}$$

$$L=l\left(\frac{\sqrt{3}}{2\pi}\right)^{1/2}\left(\frac{E^*}{\pi wR^2}\right)^{1/3} \tag{15}$$

A parameter similar to λ was first used in Ref. [5]; this parameter specifies the characteristics of adhesive

interaction of elastic spheres. The adhesion parameter λ is related to the parameter μ_T introduced by Tabor [50] as

$$\lambda = \frac{16}{9^{2/3}3^{1/2}(2\pi)^{1/3}}\mu_T \approx 1.1\mu_T \quad (16)$$

The parameter L characterizes the mutual effect of the asperities. For large values of L, the mutual effect is insignificant.

2.4 Results of calculations

For the calculations, we use Eqs. (5)–(8) with the parametrization given by Eqs. (13)–(15), which allow us to prescribe the values of the parameters λ and L. These are used to calculate the dimensionless distance d^* between the interacting surfaces for various values of the dimensionless nominal pressure p^*. The results obtained are shown in Fig. 2.

The results are presented in the domain of negative values of the nominal pressure, because in this domain, the effect of the adhesive forces is very significant. The results indicate that the adhesion parameter λ significantly affects the dependence of the nominal pressure on the distance. An increase in the parameter λ leads to a considerable increase in the values of negative nominal pressures at which the surfaces can be in contact. A decrease in the parameter L, which characterizes the distance between asperities, leads to an increase in the pull-off pressure (maximum absolute value of the negative pressure at which the contact exists) and a shift of this value to the direction of smaller distances between the interacting bodies. Thus, surfaces with asperities located closer to each other can sustain higher values of negative pressure in contact.

In an adhesive contact of elastic bodies, the work required to separate contacting surfaces from each other is in general, higher than the work done in approaching the surfaces from infinity to the initial distance. Thus, hysteresis takes place in the approach–separation cycle. This follows from the ambiguity of the curves of the nominal pressure vs distance, which can be observed for sufficiently large values of the adhesion parameter λ. When the surfaces move away from each other, the contact breaks at point A with a jump to point B. When the surfaces approach each other, a jump in contact occurs from C to D. The difference between the values of the work in the approach and separation of the surfaces is equal to the dashed area in Fig. 2; it can be calculated in accordance with the relation

$$\Delta w = \int_{ABCD} p(d)\,\mathrm{d}d \quad (17)$$

Graphs of the dimensionless energy dissipation in the approach–separation cycle vs the adhesion parameter λ are shown in Fig. 3. The energy dissipation per unit area is calculated in dimensionless form:

$$\Delta w^* = \Delta w \frac{4l^2}{3\sqrt{3}}\left(\frac{E^{*2}}{\pi^5 w^5 R^4}\right)^{1/3}.$$

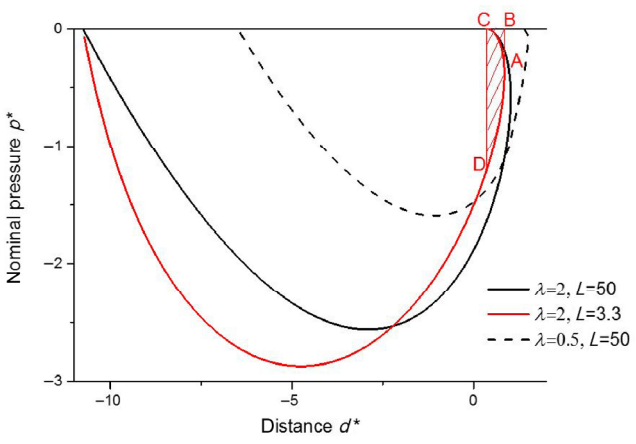

Fig. 2 Dimensionless nominal pressure vs distance in normal approach and separation of rough surfaces.

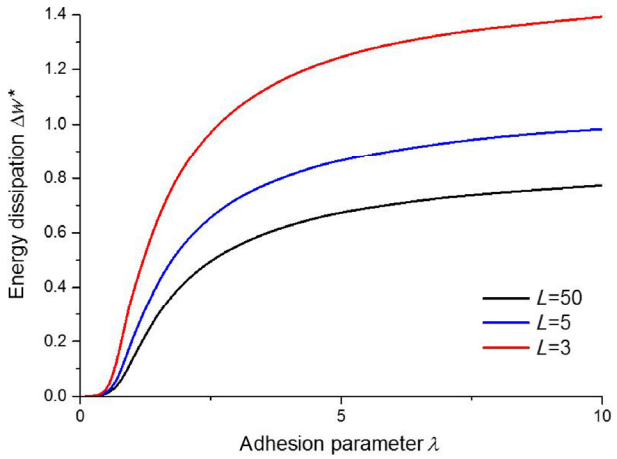

Fig. 3 Energy dissipation per unit area in the approach–separation cycle of rough surfaces.

The results indicate that the energy dissipation tends to approach zero as $\lambda \to 0$ and to a constant value as $\lambda \to \infty$. An increase in the contact density leads to an increase in the energy dissipation per unit area of the interacting surfaces.

Note that for two single elastic asperities, the analysis of the energy dissipation in an approach–separation cycle vs adhesion parameter was first carried out in Ref. [51] based on an analytical representation of the contact problem solution for the Maugis–Dugdale model of adhesion and power-law shapes of asperities. In Ref. [52], the effect of the Tabor parameter on the hysteretic loss was numerically studied for two elastic spheres interacting with the Lennard–Jones potential. The results of both these studies indicate that for smooth bodies, the dependence of the energy dissipation on the adhesion parameter is similar to that presented in Fig. 3 for a rough solid.

The obtained calculation results of the energy dissipation in the approach–separation cycle can be used to estimate the contribution of adhesion in the friction force in sliding and rolling contacts of rough surfaces.

3 Adhesion in sliding of rough surfaces

Consider the mutual sliding of two rough surfaces of regular shape. It is assumed that the upper and lower surfaces have the same period of roughness l (Fig. 4). Let surface 1 covered with asperities of radius R_1 be at rest, while surface 2, covered with asperities of radius R_2, moves in the tangential direction along the x-axis, with the vertical distance between the surfaces δ (along the z-axis) being constant. Each pair of asperities does not interact with each other initially; then, they come into contact and experience mutual sliding until the contact breaks.

To calculate the contribution of adhesive hysteretic losses into the total friction force, we assume that

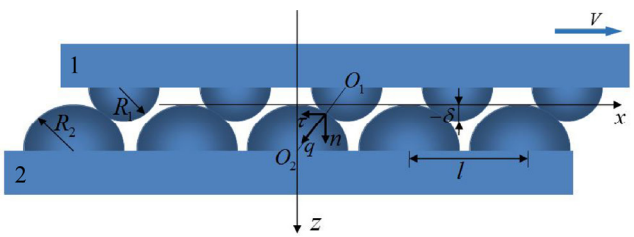

Fig. 4 Sliding scheme of two regular rough surfaces.

there is no shear stress within each contact spot. It should be also mentioned that here and in subsequent sections, the interaction of each pair of asperities is modeled separately; thus, the mutual effect of asperities is not taken into account similar to what was done in Section 2.

Because the asperities have spherical shapes, the force of interaction between them acts along the line O_1O_2 passing through the centers of the spheres. The tangential stresses are assumed to be zero; hence, the contact problem for two asperities is axisymmetric with respect to the line O_1O_2 at each instant of time. The force of interaction q as a function of the distance between two asperities d is defined by Eqs. (10) and (11) for the case involving contact between asperities and by Eq. (12) for the case with no contact. The force q can be divided into normal n and tangential τ components:

$$n = \frac{q(R_1 + R_2 + \delta)}{\sqrt{(R_1 + R_2 + \delta)^2 + x^2}}, \quad \tau = \frac{qx}{\sqrt{(R_1 + R_2 + \delta)^2 + x^2}} \tag{18}$$

where x is the tangential displacement of surface 1 with respect to surface 2.

Graphs of the dimensionless normal $n/(\pi R^* w)$ and tangential $\tau/(\pi R^* w)$ forces acting on an asperity of surface 1 during sliding along the x-axis are shown in Fig. 5. The results are obtained for the following values of the parameters characterizing the elastic and adhesive properties of the surfaces: $w/(p_0 R^*) = 0.1$ and $p_0/E^* = 0.5$. Here, R^* and E^* are the reduced radius of the asperities and elastic modulus, respectively:

$$\frac{1}{R^*} = \frac{1}{R_1} + \frac{1}{R_2}, \quad \frac{1}{E^*} = \frac{1-\nu_1}{E_1} + \frac{1-\nu_2}{E_2}.$$

The ratio of the reduced radius of the asperities to the distance between them is taken as $R^*/l = 0.3$. The curves shown in Figs. 5(a) and 5(b) correspond to the dimensionless vertical distance between the surfaces $\delta/R^* = -0.1$ and $-\delta/R^* = -0.3$, respectively. The results indicate that in the process of sliding, the tangential force τ changes its sign from positive (acting in the direction of sliding) to negative (acting in the direction opposite to sliding). Based on the obtained relations from Eqs. (10)–(12) and (18), we calculate the

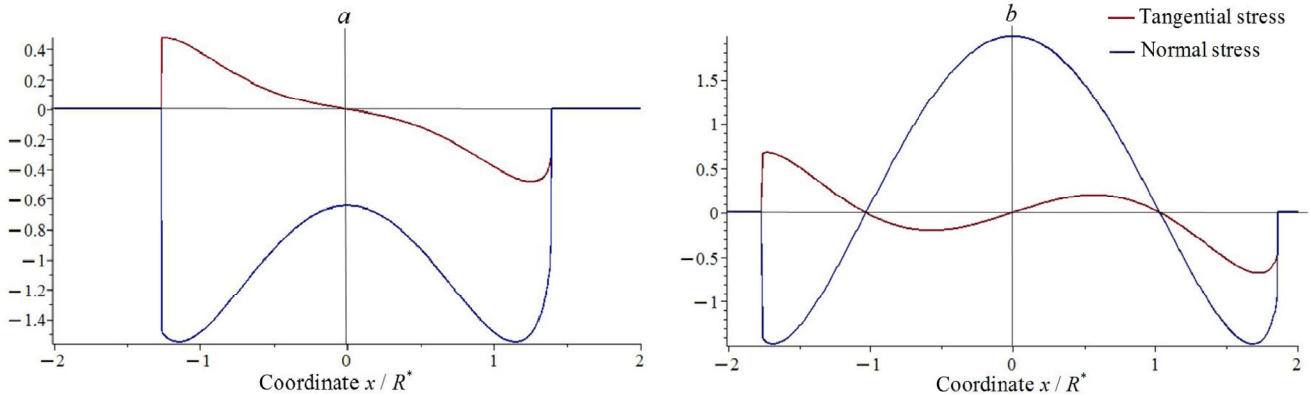

Fig. 5 Normal and tangential forces between two asperities in the sliding of two rough surfaces.

average normal and tangential forces acting on a unit area of surface 1 from surface 2:

$$T = \frac{1}{l}\int_{-l/2}^{l/2} \tau(s)\mathrm{d}s\,, \quad P = \frac{1}{l}\int_{-l/2}^{l/2} n(s)\mathrm{d}s.$$

The mean tangential force T is not equal to zero because of the energy dissipation occurring in the approach–separation cycle of asperities. This force, which is associated with the energy losses in the formation and breaking of adhesive bonds, can be called the adhesive component of the friction force. The coefficient of friction is defined by the relation

$$\mu = \frac{T}{P}.$$

Graphs of the coefficient of friction μ vs the dimensionless nominal pressure $P/(\pi E^* l^2)$ are shown in Fig. 6 for various values of the dimensionless reduced radius of asperities R^*/l for $w/(p_0 R^*) = 0.1$ and $p_0 / E^* = 1$. It is observed that the coefficient of friction increases with decreasing nominal pressure, and it attains considerably high values at very small pressures. This behavior is a characteristic of the adhesive component of the friction force. An increase in the radius of the surface asperities leads to an increase in the coefficient of friction.

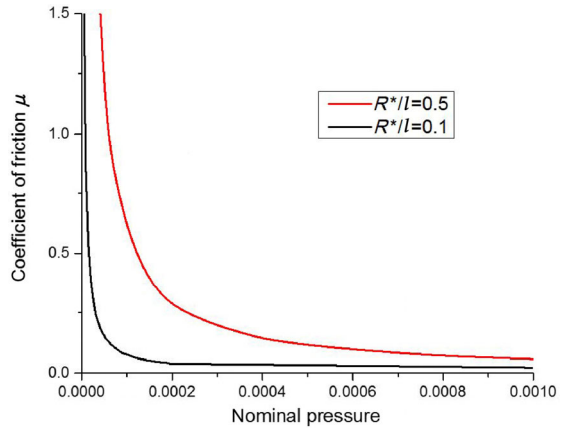

Fig. 6 Coefficient of friction vs nominal pressure.

4 Adhesive resistance to rolling of rough bodies

Consider a rigid rough cylinder of radius R rolling on the boundary of an elastic half-space (Fig. 7). The cylinder is acted upon by a normal force P and is rolling with an angular velocity ω. The surface of the cylinder is covered with a periodic system of rigid asperities located in the nodes of the rectangular lattice with spacing l. The height distribution of the asperities is described by the function $\phi(t)$. All asperities have the same radius R_0.

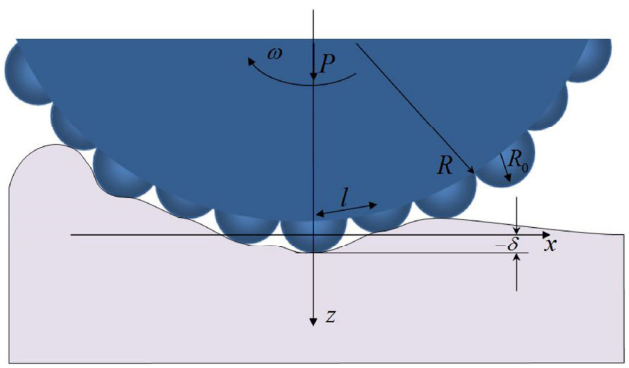

Fig. 7 Rolling scheme of a rough cylinder on an elastic half-space.

The problem is considered in the moving system of coordinates, whose *z*-axis passes through the axis of the cylinder and is directed in the half-space. Meanwhile, the *x*-axis coincides with the undeformed surface of the elastic half-space and is directed in the direction of motion of the cylinder. The value of the gap between the surfaces of the rough cylinder and the elastic half-space is defined by the expression

$$h(x,y) = u(x,y) + f(x,y) + \delta,$$

where $u(x,y)$ is the elastic displacement of the surface of the half-space in the z direction, $f(x,y)$ is a function describing the shape of the surface of the rough cylinder, and δ is the normal distance between the cylinder and the half-space.

The cylinder and the half-space are in contact over the areas of real contact A_i, in which the condition of contact is satisfied:

$$h(x,y) = 0, \quad (x,y) \in A_i.$$

The tangential stresses on the real areas of contact are assumed to be zero. The surfaces of the cylinder and half-space are attracted to each other owing to adhesion. The adhesion attraction takes place in the areas B_i, which are either ring-shaped surrounding the real contact areas A_i, or circular for asperities that are not in contact with the half-space. The dependence of the adhesive force on the gap between the surfaces is described by the piecewise constant function defined by Eq. (1). Thus, the adhesive pressure $p_a(x,y)$ on the surface of the elastic half-space is defined by

$$p_a(x,y) = \begin{cases} -p_0, & h(x,y) \le h_0 \\ 0, & h(x,y) > h_0 \end{cases}, \quad (x,y) \in B_i.$$

The work of adhesion is defined by Eq. (2).

During rolling, each *i*-th asperity approaches the surface of the elastic half-space beginning from a distance δ_∞, at which surfaces do not attract, to a minimum distance $\delta_0^{\,i}$, which occurs in the point of maximum loading of the nominal contact area. Afterward, the asperity moves away from the surface of the half-space up to the distance δ_∞. It was shown in Section 2 that in the approach–separation cycle of an asperity and the elastic half-space, energy dissipation occurs (dashed region in Fig. 2). For an asperity that passes through the contact zone in the rolling of a rough cylinder, the energy dissipation is calculated as

$$\Delta w = \int_{\delta^{\text{app}}}^{\delta^{\text{sep}}} \left[q_i^{\text{app}}(\delta) - q_i^{\text{sep}}(\delta) \right] \mathrm{d}\delta \tag{19}$$

where $q_i^{\text{app}}(\delta)$ is the force–distance dependence in the approach (branch BCD in Fig. 2) and $q_i^{\text{sep}}(\delta)$ is the force–distance dependence in the separation (branch DAB in Fig. 2). The energy dissipation as defined by Eq. (19) differs from zero under the condition that the minimum distance between the surfaces is smaller than the distance at which they come into contact (point *C* in Fig. 2). This value is denoted as δ^{app}.

As the cylinder makes a full revolution, the energy dissipation will be equal to $\Delta w N_1$, where N_1 is the number of asperities for which the minimum distance to the half-space for a full revolution of the cylinder is smaller than δ^{app}. It is assumed that this energy loss is equal to the work of the moment of rolling resistance per one revolution $2\pi M$. Then, the moment of rolling resistance can be expressed as

$$M = \frac{\Delta w N_1}{2\pi}.$$

For a model of a rough cylinder having N asperities of the same height in the cross-section, the number N_1 is defined by the following stepwise function:

$$N_1 = \begin{cases} N, & c \ge c^{\text{app}} \\ 0, & c < c^{\text{app}} \end{cases}.$$

We can also consider a case where the asperities have a statistical distribution of heights:

$$N_1 = N \int_{-\infty}^{c} \varphi(t)\mathrm{d}t.$$

where $\varphi(t)$ is the density of distribution, for example, according to the Gauss law:

$$\varphi(t) = \frac{1}{\sqrt{2\pi}\sigma} \mathrm{e}^{-\frac{1}{2}\frac{t^2}{\sigma^2}}.$$

The graphs of the dimensionless moment of rolling resistance $\dfrac{M}{E^* R^3}$ vs the dimensionless distance bet-

ween the cylinder and the half-space are shown in Fig. 8 for the one-level roughness model (curve 1) and Gaussian distribution of heights of asperities (curve 2). The results are obtained for $\frac{w}{p_0 R_0} = 0.1$, $\frac{p_0}{E^*} = 0.1$, $\frac{R_0}{R} = 0.01$, and $N = 10,000$; the mean square deviation for the case of a Gaussianian height distribution is $\frac{\sigma}{R} = 0.01$. The results indicate that as the distance between the surfaces decreases (the indentation of the cylinder into the half-space increases), the rolling resistance increases sharply in the case of one-level roughness and smoothly in the case of height distribution. At large indentations of the cylinder into the elastic half-space, the rolling resistance tends to approach a constant value that depends on the geometrical characteristics of the cylinder, elastic properties of the half-space, and characteristics of adhesion.

The results obtained indicate also that the moment of rolling resistance $\frac{M}{E^* R^3}$ increases as the work of adhesion w increases. This is illustrated by the graphs shown in Fig. 9, which are obtained for $\frac{p_0}{E^*} = 0.1$, $N = 10,000$, and various radii of curvature of asperities $\frac{R_0}{R} = 0.01$ (curve 1) and $\frac{R_0}{R} = 0.012$ (curve 2) for the case of asperities of the same height and when the distance between the cylinder and the half-space is smaller than δ^{app}. It is evident that the moment of rolling resistance tends to approach a constant value as the work of adhesion increases, which is the result

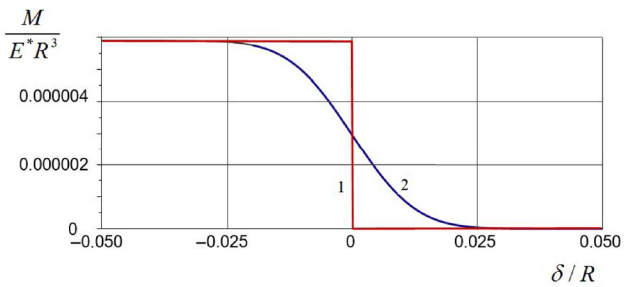

Fig. 8 Moment of rolling resistance vs dimensionless distance between a cylinder and elastic half-space.

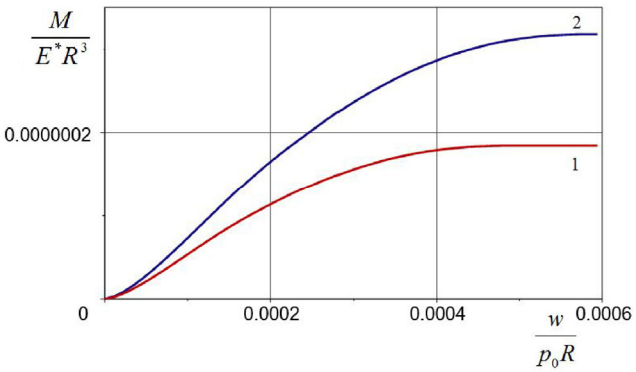

Fig. 9 Moment of rolling resistance vs dimensionless work of adhesion.

of using the simplified Maugis–Dugdale model as defined by Eq. (1), to describe the adhesive interaction of the surfaces instead of the full Lennard–Jones form. It also follows from the results that the adhesive losses of energy and hence, the rolling resistance, are higher for asperities with larger radius R_0.

5 Conclusion

In this study, an approach is developed to investigate the combined effect of the parameters of adhesive interaction and surface microgeometry on the contact characteristics and energy dissipation in an approach–separation cycle of elastic bodies with regular surface relief, as well as in their mutual sliding and rolling.

The load–distance dependence and the energy dissipation in the approach–separation cycle are calculated for two elastic bodies, one of which is covered with a periodic system of asperities of spherical shape, by taking into account the forces of both elastic compression and adhesive attraction between the surfaces. The mutual effect of microcontacts was taken into account, making it possible to establish the dependence of the characteristics in question on the shape and density of the asperities and the parameters of adhesion.

A method is developed to calculate the adhesive component of the friction force in the conditions of mutual sliding and rolling of elastic bodies with regular surface microgeometry. The method is based on the determination of the energy dissipation in the

approach–separation cycle of asperities. Based on the model calculations performed, the dependencies of the coefficient of friction on the nominal pressure are established for various values of the parameters of roughness and adhesion.

The results obtained can be applied for controlling the microgeometric parameters of dry surfaces to attain the required frictional characteristics on specified regimes of interaction.

Acknowledgment

This work was carried out under the financial support of the Russian Science Foundation (grant No. 14-29-00198). The authors are also grateful for the discussion within the framework of the CARBTRIB International network supported by the Leverhulme Trust.

References

[1] Tomlinson J A. A molecular theory of friction. *Philos Mag* **46**: 905–939 (1929)

[2] Derjaguin B. Molekulartheorie der äußeren Reibung. *Z Phys* **88**: 661–164 (1934)

[3] Johnson K L, Kendall K, Roberts A D. Surface energy and the contact of elastic solids. *Proc Roy Soc Lond* A **324**: 301–313 (1971)

[4] Derjaguin B V, Muller V M, Toporov Y P. Effect of contact deformations on the adhesion of particles. *J Colloi. Interface Sci* **53**(2): 314–326 (1975)

[5] Maugis D. Adhesion of spheres: The JKR-DMT transition using a Dugdale model. *J Colloid Interface Sci* **150**: 243–269 (1992)

[6] Greenwood J A. Adhesion of elastic spheres. *Proc Roy Soc Lond A* **453**: 1277–1297 (1997)

[7] Barthel E. On the description of the adhesive contact of spheres with arbitrary interaction potentials. *J Colloid Interface Sci* **200**: 7–18 (1998)

[8] Greenwood J A, Johnson K L. An alternative to the Maugis model of adhesion between elastic spheres. *J Phys D-Appl Phys* **31**(22): 3279–3290 (1998)

[9] Goryacheva I G, Makhovskaya Y Y. An approach to solving the problems on interaction between elastic bodies in the presence of adhesion. *Dokl Phys* **49**(9): 534–538 (2004)

[10] Johnson K L. Non-Hertzian contact of elastic bodies. In *The Mechanics of the Contact Between Deformable Bodies*. Pater D E, Kalker J J, Eds. Delft University Press, 1975: 26–40.

[11] Fuller K N G, Tabor D. The effect of surface roughness on the adhesion of elastic solids. *Proc Roy Soc London A* **345**: 327–342 (1975)

[12] Maugis D. *Contact, Adhesion and Rupture of Elastic Solids*. Berlin: Springer-Verlag, 2000.

[13] Morrow C, Lovell M, Ning X. A JKR-DMT transition solution for adhesive rough surface contact. *J Phys D* **36**: 534–540 (2003)

[14] Galanov B A. Models of adhesive contact between rough elastic bodies. *Int J Mech Sci* **53**: 968–977 (2011)

[15] Rumpf H. *Particle Technology*. London: Chapman & Hall, 1990.

[16] Rabinovich Y I, Adler J J, Ata A, Singh R K, Moudgil B M. Adhesion between nano-scale rough surfaces: I. Role of asperity geometry. *Journal of Colloid and Interface Science* **232:** 10–16 (2000)

[17] Derjaguin B. Untersuchungen uber die Reibung und Adhasion, IV. Theorie des Anhaftens kleiner Teilchen. *Kolloid Zeitschrift* **69:** 155–164 (1934)

[18] Borodich F M. The Hertz-type and adhesive contact problems for depth-sensing indentation. *Advances in Applied Mechanics* **47**: 225–366 (2014)

[19] Popov V L, Filippov A E. Adhesive properties of contacts between elastic bodies with randomly rough self-affine surfaces: A simulation with the method of reduction of dimensionality. *Phys Mesomech* **15**(5): 324–329 (2012)

[20] Sahoo P, Chowdhury S K R. A fractal analysis of adhesion at the contact between rough solids. *Proc. Instn. Mech. Engrs*. **210**: 269–279 (1996)

[21] Persson B N J, Tossati E. The effect of surface roughness on the adhesion of elastic solids. *J Chem Phys* **115**: 5597–5610 (2001)

[22] Persson B N J. Adhesion between elastic bodies with randomly rough surfaces. *Phys Rev Lett* **89**: 245502-1-245502-4 (2002)

[23] Persson B N, Scaraggi M. Theory of adhesion: Role of surface roughness. *J Chem Phys* **141**(12): 124701 (2014)

[24] Ciavarella M. Adhesive rough contacts near complete contact. *International Journal of Mechanical Sciences* **104**: 104–111 (2015)

[25] Pastewka L, Robbins M O. Contact between rough surfaces and a criterion for macroscopic adhesion. *Proceedings of the National Academy of Sciences* **111**(9): 3298–3303 (2014)

[26] Ciavarella M. On Pastewka and Robbins' criterion for macroscopic adhesion of rough surfaces. *Journal of Tribology* **139**(3): 031404 (2017)

[27] Ciavarella M. On the use of DMT approximations in adhesive contacts, with remarks on random rough contacts. *Tribology International* **114**: 445–449 (2017)

[28] Ciavarella M. A very simple estimate of adhesion of hard solids with rough surfaces based on a bearing area model. *Meccanica*, DOI 10.1007/s11012-017-0701-6 (2017)

[29] Borodich F M. Fractal contact mechanics. In: *Encyclopedia of Tribology*. Wang Q J, Chung Y-W (Eds.). Springer, 2013: 1249–1258.

[30] Borodich F M, Pepelyshev A, Savencu O. Statistical approaches to description of rough engineering surfaces at nano and microscales. *Tribology International* **103**: 197–207 (2016)

[31] Hui C Y, Lin Y Y, Baney J M, Kramer E J. The mechanics of contact and adhesion of periodically rough surfaces. *J Polym Sci B* **39**: 1195–1214 (2001)

[32] Adams G G. Adhesion at the wavy contact interface between two elastic bodies. *ASME J Appl Mech* **71**(6): 851–856 (2004)

[33] Chumak K. Adhesive contact between solids with periodically grooved surfaces. *Int J Solids Struct* **78**: 70–76 (2016)

[34] Makhovskaya Y Y. Discrete contact of elastic bodies in the presence of adhesion. *Mech Solids* **38**(2): 39–48 (2003)

[35] Bowden F P, Tabor D. *Friction and Lubrication of Solids*. Oxford (UK): Oxford University Press, 1950.

[36] Chowdhury S K, Roy Ghosh P. Adhesion and adhesional friction at the contact between solids. *Wear* **174**: 9–19 (1994)

[37] Kogut L, Etsion I. Static friction model for elastic-plastic contacting rough surfaces. *J Tribol-T ASME* **126**: 34–40 (2004)

[38] Sahoo P, Mitra A, Saha K. Elastic-plastic adhesive contact of rough surfaces using n-Point asperity model. *J Phys D: Appl Phys* **42**: 1–13 (2009)

[39] Johnson K L. Adhesion and friction between a smooth elastic spherical asperity and a plane surface. *Proc R Soc. Lond A* **453**: 163–179 (1997)

[40] Chaudhury M K, Owen M J. Adhesion hysteresis and friction. *Langmuir* **9**(1): 29–31 (1993)

[41] Szoszkiewicz R, Bhushan B, Huey B D, Kulik A J, Gremaud G. Correlations between adhesion hysteresis and friction at molecular scales. *The Journal of Chemical Physics* **122**(14) (2005)

[42] Yoshizawa H, Chen Y-L, Israelachvili J. Fundamental mechanisms of interfacial friction. 1. Relation between adhesion and friction. *J Physical Chemistry* **97**(16): 4128–4140 (1993)

[43] Barquins M. Adherence, friction and contact geometry of a rigid cylinder rolling on the flat and smooth surface of an elastic body. *J Nat Rub Rs* **5**(3): 199–210 (1990)

[44] Carbone G, Mangialardi L. Adhesion and friction of an elastic half-space in contact with a slightly wavy rigid surface. *Journal of the Mechanics and Physics of Solids* **52**(6): 1267–1287 (2004)

[45] Heise R, Popov V L. Adhesive contribution to the coefficient of friction between rough surfaces. *Tribology Letters* **39**(3): 247–250 (2010)

[46] Goryacheva I, Makhovskaya Y. A model of the adhesive component of the sliding friction force. *Wear* **270**: 628–633 (2011)

[47] Derjaguin B V, Krotova N A, Smilga V P. *Adhesion of Solids*. London: Consultants Bureau, 1978.

[48] Goryacheva I G, Makhovskaya Y Y. Adhesive resistance in the rolling of elastic bodies. *J Appl Math Mech* **71**(4): 485–493 (2007)

[49] Goryacheva I G. *Contact Mechanics in Tribology*. Dordreht: Kluwer Academic Publishers, 1997.

[50] Tabor D. Surface forces and surface interactions. *J Colloids Interface Sci* **58**(2): 2–13 (1977)

[51] Goryacheva I G, Makhovskaya Y Y. Adhesive interaction of elastic bodies. *Journal of Applied Mathematics and Mechanics* **65**(2): 273–282 (2001)

[52] Ciavarella M, Greenwood J A, Barber J R. Effect of Tabor parameter on hysteresis losses during adhesive contact. *Journal of the Mechanics and Physics of Solids* **98**: 236–244 (2017)

Irina GORYACHEVA. She received her Ph.D. degree in Moscow State University in 1974 and her D. Sci degree in Institute for Problems in Mechanics of the Russian Academy of Sciences in 1988. She is the full member of the Russian Academy of Sciences since 2003. Her current position is a professor of the Moscow State University and Moscow Institute of Physics and Technology, head of the Tribology Laboratory at Institute for Problems in Mechanics. Her research interests cover a broad range of problems in contact mechanics and tribology.

Yulia MAKHOVSKAYA. She received her Ph.D. degree in Institute for Problems in Mechanics of the Russian Academy of Sciences in 2001. Her current position is a senior researcher in the Tribology Laboratory at Institute for Problems in Mechanics. Her research interests lie in modeling the interaction of elastic and viscoelastic bodies taking into account adhesion.